Energy Conversion and Management: X 30 (2026) 101750

Contents lists available at ScienceDirect

Energy Conversion and Management: X

journal homepage: www.sciencedirect.com/journal/energy-conversion-and-management-x

Optimizing interoperable hydrogen supply chain design: A case study in Auvergne-Rhône-Alpes

Renato Luise [a,b,*], Catherine Azzaro-Pantel [b], Annabelle Brisse [c]

[a] European Institute for Energy Research, Emmy-Noether Straße 11, Karlsruhe, 76131, Germany
[b] Université Toulouse, Laboratoire de Génie Chimique, CNRS, INPT, UPS, 6 Allée Emile Monso, Toulouse, 31400, France
[c] Hynamics, 8-10 avenue de l'ARCHE – Immeuble le Colisée – Bâtiment C, Courbevoie, 92400, France

ARTICLE INFO

Keywords:
Hydrogen supply chain
Decarbonization of energy market
Novel superstructure
Optimization

ABSTRACT

Low-carbon hydrogen is a key enabler of the energy transition, yet the optimal design of hydrogen supply chains remains uncertain in terms of cost and emissions. This study analyzes the trade-offs between centralized and decentralized hydrogen production and storage by proposing a novel superstructure integrating advanced production, storage, transport, and conditioning technologies. A spatial, multi-period mixed-integer linear programming optimization model is developed to minimize the Levelized Cost of Hydrogen (LCOH) while quantifying direct (on-site) CO_2 emissions along the supply chain.

The model is applied to the Auvergne-Rhône-Alpes region in France. Results indicate that centralized hydrogen production based on steam methane reforming with carbon capture and storage achieves the lowest costs but results in higher emissions compared to electrolysis-based pathways. The cost-optimal configuration delivers hydrogen at an average LCOH of 4.0 €/kgH_2 with emissions of 1.60 kgCO_2eq/kgH_2, whereas the emissions-oriented configuration reduces emissions to 0.15 kgCO_2eq/kgH_2 at an increased cost of 6.2 €/kgH_2.

Sensitivity analyses show that lower hydrogen demand initially favors decentralized configurations, reducing short-term costs, but leads to higher long-term LCOH once investments are amortized. A 20% reduction in capital costs has a stronger impact on refueling stations (−5.5%) than on production facilities (−1.6%). Under high energy price scenarios, LCOH increases by 55.3%, favoring supply chain designs that prioritize local resource utilization and hydrogen transport from renewable-rich to constrained areas.

Future work will address demand and renewable supply uncertainties through stochastic modeling, extend the superstructure to additional technologies, and assess deployment pathways from regional to national scales.

1. Introduction

Low-carbon hydrogen is widely acknowledged as a key enabler of the energy transition and the decarbonization of the industrial and mobility sectors [1]. National and international roadmaps predict a substantial increase in hydrogen production and use in various applications by 2050 [2]. However, unlocking the full potential of hydrogen depends critically on the ability to design efficient, cost-effective, low-emission, and interoperable supply chains that can coordinate multiple technologies and infrastructures across varying territorial, technological, and sectoral contexts. Recent studies emphasize that the integration of spatially-resolved infrastructure and detailed supply chain modeling is critical for assessing techno-economic and environmental trade-offs [3–5].

Among the most pressing challenges facing hydrogen supply chain (HSC) development are strategic choices related to system architecture, particularly the degree of centralization in production and storage facilities, and the resulting implications for cost, flexibility, interoperability, and emissions. Hydrogen can be produced in large centralized units, such as Steam Methane Reforming (SMR) plants or utility-scale electrolyzers, offering economies of scale but requiring long-distance transport. Alternatively, decentralized, on-site production (e.g., electrolysis at refueling stations) can reduce transport needs and offer higher flexibility, albeit with typically higher unit costs and integration complexity [6]. Recent analyses of supply chain resilience highlight the importance of considering both transport modalities and multi-option flexibility in recent HSC designs [7].

Storage plays a pivotal role in these architectural choices. Centralized storage facilities, usually co-located with production plants, enable large-volume buffering and distribution to multiple demand sites. In contrast, decentralized storage, located at or near end-user facilities,

* Corresponding author at: European Institute for Energy Research, Emmy-Noether Straße 11, Karlsruhe, 76131, Germany.
E-mail address: renato.luise@eifer.org (R. Luise).

https://doi.org/10.1016/j.ecmx.2026.101750
Received 4 July 2025; Received in revised form 30 January 2026; Accepted 5 March 2026
Available online 6 March 2026

ensures local availability and operational autonomy, which is especially valuable under variable demand conditions or in remote regions. The interplay between these two storage strategies significantly influences the design, cost, and environmental impact of the overall HSC. Recent literature has also incorporated GIS-based modeling and spatial optimization to better represent the effects of storage location on cost and emissions [8,9].

While prior modeling efforts often analyze centralized and decentralized configurations separately, this work introduces a comprehensive and innovative superstructure that captures the full spectrum of centralized, decentralized, and hybrid production-storage combinations. A key novelty is the explicit modeling of intersite interactions between decentralized production and storage units, enabling interoperability across the system so that hydrogen produced in excess at one location can be redistributed to neighboring nodes. This flexible coordination between geographically distributed units supports operational resilience and facilitates efficient integration of diverse hydrogen technologies under variable demand conditions, which is particularly critical during early deployment phases.

In addition to these architectural features, the proposed framework explicitly integrates multi-sectoral demand (mobility and industry), spatially resolved infrastructure, and the temporal evolution of hydrogen deployment from 2025 to 2050. This combination of configurational, spatial, and temporal dimensions enables the assessment of context-specific trade-offs between cost and emissions. By unifying techno-economic and environmental objectives within an interoperable superstructure, the proposed approach moves beyond generic HSC modeling to address practical challenges associated with regional implementation. This positioning is consistent with recent advances in multi-sectoral hydrogen integration and scenario analysis [4,10].

The proposed superstructure is structured around four functional pillars: production, storage, transport, and usage, and it is scalable both territorially (from regional to national levels) and sectorally (covering mobility and industry). It supports a unified mathematical optimization framework integrating both techno-economic and environmental criteria, namely the Levelized Cost of Hydrogen (LCOH) and Global Warming Potential (GWP).

Building on foundational works in process and energy systems optimization [11–16], our model significantly expands existing capabilities by accounting for diverse technology readiness levels (TRLs), conditioning options, and transport modalities (pipeline vs. road). This interoperability-driven integration enables the representation of a broader set of realistic deployment scenarios, where technological maturity, infrastructure availability, and spatial constraints jointly influence supply chain design. By capturing these interdependencies, the model allows for a nuanced analysis of the trade-offs between economies of scale — typically associated with centralized configurations — and the adaptability and resilience provided by more decentralized systems.

The central research question addressed in this work is: how can a flexible, multi-level HSCs be designed to simultaneously minimize cost and emissions, while balancing centralized and decentralized storage and production strategies and ensuring system-wide interoperability?

Applied to the Auvergne-Rhône-Alpes (ARA) region, the model demonstrates how regional characteristics, energy availability, and sectoral demand shape optimal supply chain designs. This region-specific application underscores the added value of the proposed framework beyond generic HSC studies, while providing a reusable approach for future regional planning and decision-making.

The remainder of this paper is structured as follows. Section 2 introduces the proposed superstructure-based modeling framework and outlines a classification of existing HSC configurations, with a focus on production and storage centralization. Section 3 presents the optimization model, detailing the technological assumptions and the performance indicators used, namely the LCOH and the GWP. Section 4 applies the model to a real-world case study in the Auvergne-Rhône-Alpes (ARA) region of France, providing a comparative analysis of design scenarios and associated trade-offs. Finally, Section 5 discusses the strategic implications of the findings and suggests directions for future research, particularly the integration of stochastic elements to address uncertainties in demand and renewable energy availability.

2. Literature review for classification of hydrogen supply chain superstructures

HSC design has been extensively studied, with many contributions proposing optimization-based models, typically formulated as mixed-integer linear programming (MILP) problems to configure production facilities, transportation modes, and hydrogen flow allocations. Multi-objective and multi-period frameworks have been introduced to capture trade-offs among economic, environmental, and safety criteria under demand and supply uncertainties. Some studies also integrate HSC design with complementary systems such as renewable energy generation, power-to-gas, ammonia synthesis, and electricity grids [3,8,10,17].

Although these works provide valuable insights into technological pathways and operational optimization, few explicitly address the structural architecture of hydrogen supply networks, particularly regarding the spatial configuration and centralization of production plants and storage. Only a limited number of studies examine how interconnections between alternative production, storage, and distribution topologies influence system-wide performance in terms of cost, environmental impact, and flexibility. This gap highlights the need for a systematic understanding of how different logistical designs and the interoperability of various options shape the feasibility and scalability of hydrogen deployment strategies.

2.1. Framework and typology

Based on a comprehensive literature review, we propose a classification framework grounded in a systemic analysis of hydrogen logistics. The framework is organized around the four fundamental pillars of supply chains: *production*, *storage*, *transportation*, and *usage*. It deliberately abstracts from specific technologies and mathematical formulations to emphasize the spatial and functional organization of supply chain components.

The classification distinguishes HSC superstructures according to the degree of centralization of production and storage systems. Four representative superstructures were identified, each corresponding to a distinct logistical arrangement:

- **Superstructure 1: Centralized production, decentralized storage**, Fig. 1. Hydrogen is generated in a centralized facility (e.g., SMR or large-scale electrolysis) and transported to storage units located at or near demand nodes, such as hydrogen refueling stations. This configuration is prevalent in the literature (e.g., [11,12,18–22]) and typically supports decentralized autonomy in end-use systems.

- **Superstructure 2: Centralized production and centralized storage**, Figs. (2a) and 2(b). Hydrogen is both produced and stored centrally. Two sub-configurations are distinguished: (a) centralized storage located at a distinct hub, and (b) storage co-located with the production plant. Hydrogen is then distributed to demand sites. This structure is analyzed in works such as [23–30].

- **Superstructure 3: Centralized and decentralized production, centralized storage**, Figs. (3a) and 3(b). This hybrid configuration combines centralized and on-site hydrogen production with a centralized storage unit, enhancing system resilience and operational flexibility. Both spatial configurations of storage (i.e. (a) and (b)) are considered in studies [31–35].

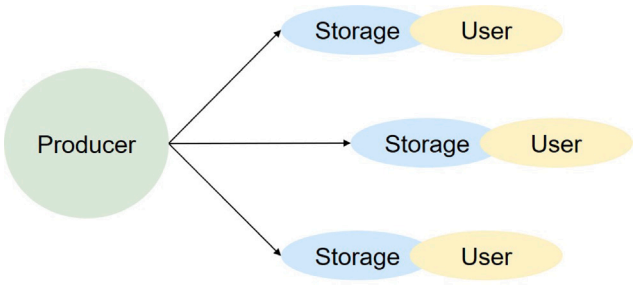

Fig. 1. Superstructure 1.

- **Superstructure 4: Centralized production, centralized and decentralized storage**, Figs. (4a) and 4(b). This architecture involves centralized hydrogen production combined with centralized storage, from which hydrogen is distributed to decentralized storage units located at the demand sites. Both storage configurations (i.e., (a) and (b)) are considered and analyzed in existing studies [36–38].

Each superstructure reflects different trade-offs in investment cost, operational complexity, supply chain robustness, and sectoral adaptability. A recurrent limitation observed in the literature is the lack of explicit justification for the chosen superstructure; structural assumptions are often implicit, embedded within case-specific scenarios. The proposed classification thus serves as a meta-framework to clarify and compare the architectural underpinnings of HSC design studies.

2.2. Generic superstructure and interoperability of the HSC components

Building upon this typology, a generic superstructure was conceptualized to encapsulate all observed configurations while supporting flexible scenario development. Inspired by recent modeling efforts such as [16,39–42], the proposed structure integrates centralized and decentralized production and storage facilities. It also includes the possibility of hydrogen reallocation among decentralized units, for example by transferring surplus hydrogen from one refueling station to another in electrolysis-based networks.

The combination of these various technical solutions, based on centralized and/or decentralized production and storage installations and their interoperability, brings us to the first output of this work: a novel superstructure for the HSC design, proposed in Fig. 5. This generic superstructure has been selected for its:

- **Configurational completeness**, enabling the representation of emerging deployment models;
- **Multi-sectoral integration**, accounting for hydrogen demand in both mobility and industrial applications—a dimension often neglected in previous studies;
- **Operational realism**, incorporating multiple pressure regimes (low-, medium-pressure), conditioning steps (compression, liquefaction), and transport modes (pipeline, tube trailer, liquid tanker).

The proposed classification not only consolidates fragmented insights across the literature but also provides a reusable and scalable framework for future optimization and decision-support models. It is intended to support strategic infrastructure planning under evolving technological and policy landscapes.

The choice between centralized and decentralized solutions remains open and is not fixed a priori. Instead, the model is designed to highlight the most appropriate configuration based on the provided inputs, system constraints, and selected optimization criteria, as shown in Fig. 6. Depending on the trade-offs involved, the optimal solution may favor large-scale centralized production, which benefits from economies of scale but incurs higher transport costs, or decentralized production, which simplifies logistics and reduces transportation needs, albeit at a higher unit production cost.

3. Model formulation and development

3.1. Implementation of a panel of hydrogen technologies

With the superstructure identified, attention can now be focused on the technical components of the model. The objective of this study is to develop a HSC, with a particular focus on energy sources that can support Low Carbon Emitting Technologies (LCETs). These technologies exhibit a lower emission intensity compared to existing alternatives [43].

The selected technologies enable the production of two distinct types of hydrogen - Renewable Hydrogen (RH) and Low Carbon Hydrogen (LCH). These hydrogen types are defined in the French Ordinance 2021-167, as amended on February 17th, 2021 [44]:

- RH is produced using renewable energy sources with a carbon threshold to be specified by decree;
- LCH is produced using low-carbon energy sources, including non-renewable sources, with the same carbon threshold defined as RH;

The European Commission has expressed its intention to set the emissions threshold at less than 70% (that is 3.38 kg_{CO_2}/kg_{H_2}) compared to current fossil fuel-based technologies, based on life cycle assessment [45]. Any hydrogen that does not fall into these categories will be considered carbon-based hydrogen.

To ensure consistency and computational tractability, a limited but representative panel of technologies has been selected. The choice was guided by technological maturity, availability of reliable data, and relevance to the European decarbonization context. Only mature and scalable solutions were retained in the model.

Alternative technologies such as Liquid Organic Hydrogen Carriers (LOHCs), ammonia, or methanol were excluded from this study, despite their potential, due to one or more of the following reasons: (i) lower technological readiness, (ii) high energy penalties during conversion cycles, or (iii) greater relevance to large-scale international trade scenarios rather than regional supply chains. The model therefore focuses on mature and scalable solutions, namely water electrolysis and SMR with CCS, while acknowledging carrier-based options as promising directions for future research.

To gain a better understanding of the flow of hydrogen and energy, the HSC has been divided into six stages, namely, primary energy source, hydrogen production, conditioning and centralized storage, distribution, conditioning and decentralized storage, and final usage. However, it is important to note that there is no singular pathway, and multiple options exist, each involving different technologies, which can lead to the final supply of hydrogen.

For **hydrogen production**, despite the availability of various technologies, only two technologies have been selected: water electrolysis and SMR with carbon capture and storage (CCS). For water electrolysis, the technical and economic inputs are based on average values for Proton Exchange Membrane (PEM) and Alkaline electrolysers, as these technologies exhibit the highest TRL (i.e. 9) and are the only options for which consistent data on installation costs and operational experience at the MW scale are available in the European context. Given this context, it is challenging to envision a HSC based on coal gasification or partial oil oxidation. While biomass gasification could offer a low-emissions solution, its TRL was deemed insufficient to be included in this study [46]. Alternative technologies, such as Autothermal Reforming (ATR), were also excluded due to lower technological maturity, limited industrial deployment in Europe, and the lack of comprehensive

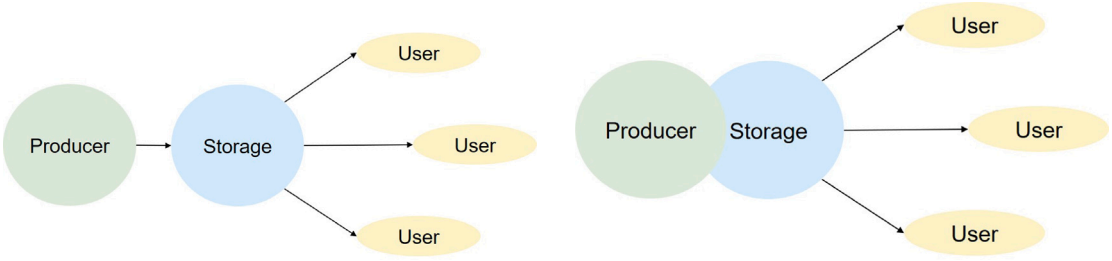

(a) Configuration a. (b) Configuration b.

Fig. 2. Superstructure 2.

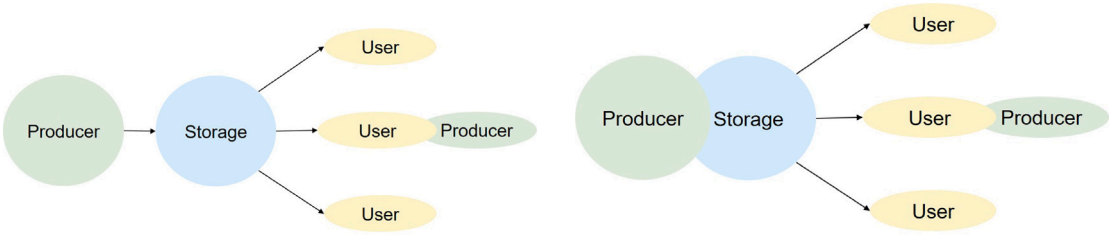

(a) Configuration a. (b) Configuration b.

Fig. 3. Superstructure 3.

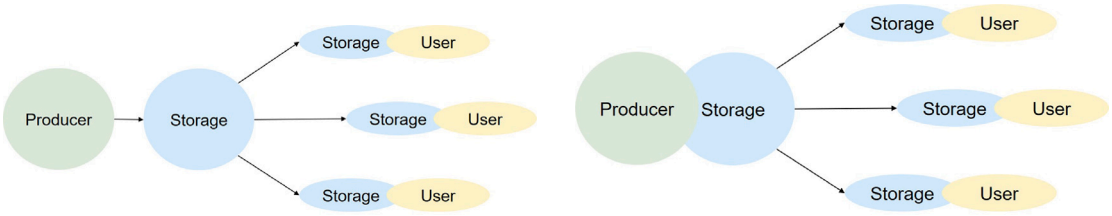

(a) Configuration a. (b) Configuration b.

Fig. 4. Superstructure 4.

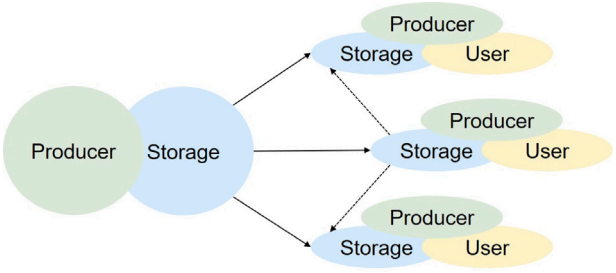

Fig. 5. Novel superstructure.

techno-economic and environmental data necessary for reliable HSC modeling. This selection ensures both computational tractability and robustness of the optimization results. A third potential source of hydrogen is imports from external systems, here referred to for simplicity as "from abroad".

Primary energy sources: Studies were conducted to assess the availability and costs of electricity for water electrolysis and auxiliary uses, and methane for SMR production. A deeper explanation of the methodology applied is provided in [47].

The hydrogen produced must undergo conditioning processes to be then stored and prepared for transport and/or use. This work primarily focused on physically-based storage systems, which are considered the most mature industrial-scale technologies, in particular liquid hydrogen and compressed hydrogen.

The sizing of the storage facilities is crucial for ensuring the reliability of both the production and supply sides. Centralized storage is sized based on the daily production capacity, while decentralized storage, located at refueling stations, is designed to make the station independent from hydrogen suppliers for several days.

Transporting hydrogen from production plants to end-users is a key aspect of the HSC and has a significant impact on the overall cost. Like storage and conditioning, transportation faces challenges such as low volumetric energy density, high molecular fugacity, and constraints related to weight and footprint. Various technical solutions address these challenges, tailored to the quantity of hydrogen and transport

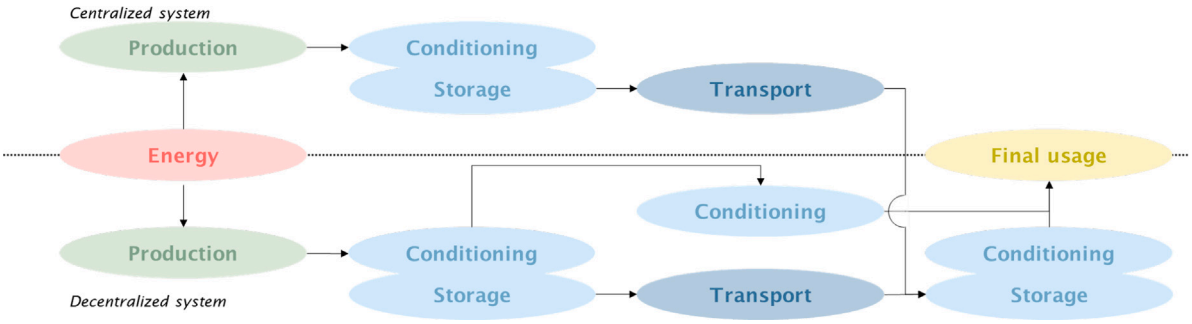

Fig. 6. Novel superstructure: centralized and decentralized systems.

distances. In addition to the solutions presented in [14] (i.e., tanker trucks for liquid hydrogen and tube trailers for compressed hydrogen) the transportation of compressed hydrogen via pipelines has been implemented in this work.

Unlike much of the existing literature, which typically focuses on transporting hydrogen from centralized plants to decentralized users, this work considers interconnected centralized and decentralized production. As a result, hydrogen can be transported from both types of plants to end users. However, this approach blurs the distinction between hydrogen transport and distribution, as noted by various authors (e.g. [24,25,27,28,33,39,48]).

At the end of the supply chain, several categories of **final users** can be identified. Hydrogen has applications in the industrial and mobility sectors, as well as in other sectors such as heat and power generation for industries, residential use, and energy storage [1].

This work will primarily focus on the demand for hydrogen in the industrial and mobility sectors.

On the one hand, the **industrial sector** already has an established market, mainly dependent on hydrogen produced from fossil fuels, which needs to be decarbonized. The global demand for hydrogen in 2023 exceeded 97 million tons (+2.5% compared to 2022) [1], with 99% of it directed at refinery processes (42%), Ammonia production (36%), Methanol production (15%) and the iron and steel industry (6%) [49].

On the other hand, the **mobility sector** represents an emerging market in need of decarbonization. The demand for hydrogen for new applications, including mobility, currently accounts for less than 1% of the global demand, but has increased by 40% since 2022 [1]. While the rise of electric vehicles is expected to dominate the sector, there is also potential for a significant low-emission hydrogen demand, projected to cover up to 30% of hydrogen demand in Europe by 2050 [2].

Fig. 7 illustrates the series of intermediate steps in the pathway from primary energy sources to the final delivery of hydrogen.

3.2. Spatial and temporal approach

Spatial approach: Building on the model introduced in [14,50], a similar approach has been adopted for both the spatial and temporal dimensions. The territory is discretized, segmenting each analyzed area into grids. Each grid is characterized by its own specific features, including the availability of primary energy sources and hydrogen demand. The optimization model decides which technologies to install in each grid, in what quantities, and during which period. It is important to emphasize that no distribution occurs between production plants and final users within the same grid; however, hydrogen can be transported from both centralized and decentralized production plants to other grids. Additionally, as per the novel superstructure introduced in the previous section, a centralized storage facility is always located near a centralized production plant, while decentralized storage is installed near hydrogen demand points associated with the mobility sector (i.e., hydrogen refueling stations).

Fig. 8 provides a simplified illustration of how installations within grids are structured.

Temporal approach: the time frame of this work is divided into five periods of 5 years each, analyzing the evolution of hydrogen demand from 2025 to 2050, aligned with the year set by the International Energy Agency (IEA) for achieving net-zero emissions. This allows the definition of a new hydrogen demand at the beginning of each period and updates the costs based on the evolution of technology costs.

3.3. Model implementation

In the literature, several mathematical approaches have been adopted by researchers to tackle HSC modeling and optimization [51].

To solve multi-period, single-objective optimization problems, various approaches and methodologies are presented in the literature. As mentioned in works such as [52], this work does not aim to provide an exhaustive explanation of all the different mathematical models and approaches developed to date.

Among the various approaches, a single-objective optimization model based on a spatial, multi-period framework has been identified as the most suitable solution and implemented in this work. The developed model aims to minimize the costs associated with the HSC, from production facilities to end-users. Additionally, as a secondary objective, it seeks to minimize local CO_2 emissions generated within the HSC, specifically those related to the use of energy sources. The model follows a deterministic approach, where hydrogen demand is predefined and must be met. The implementation is carried out in the GAMS environment, and the optimization problem, formulated as a MILP model, is solved using the CPLEX solver. Only the main improvements, categorized according to different levels of the HSC, are presented in this Section.

Energy source constraints

Each energy source e (i.e. renewable from re-powered plants, renewable from new installed plants, non-renewable energy, methane, hydrogen) has a specific availability in each grid g at the beginning of each time period t, denoted as A0(e,g,t). Taking into account the energy consumption coefficient γ_{epj} of each production plant and the production rate PR of each plant p of size j in grid g at time t, the remaining available energy is calculated to ensure that the total energy consumed does not exceed the available energy (see also non-negative constraints):

$$A_{egt} = A0_{egt} - \sum_{pji} \gamma_{epj} PR_{epjigt} \quad \forall e, g, t \tag{1}$$

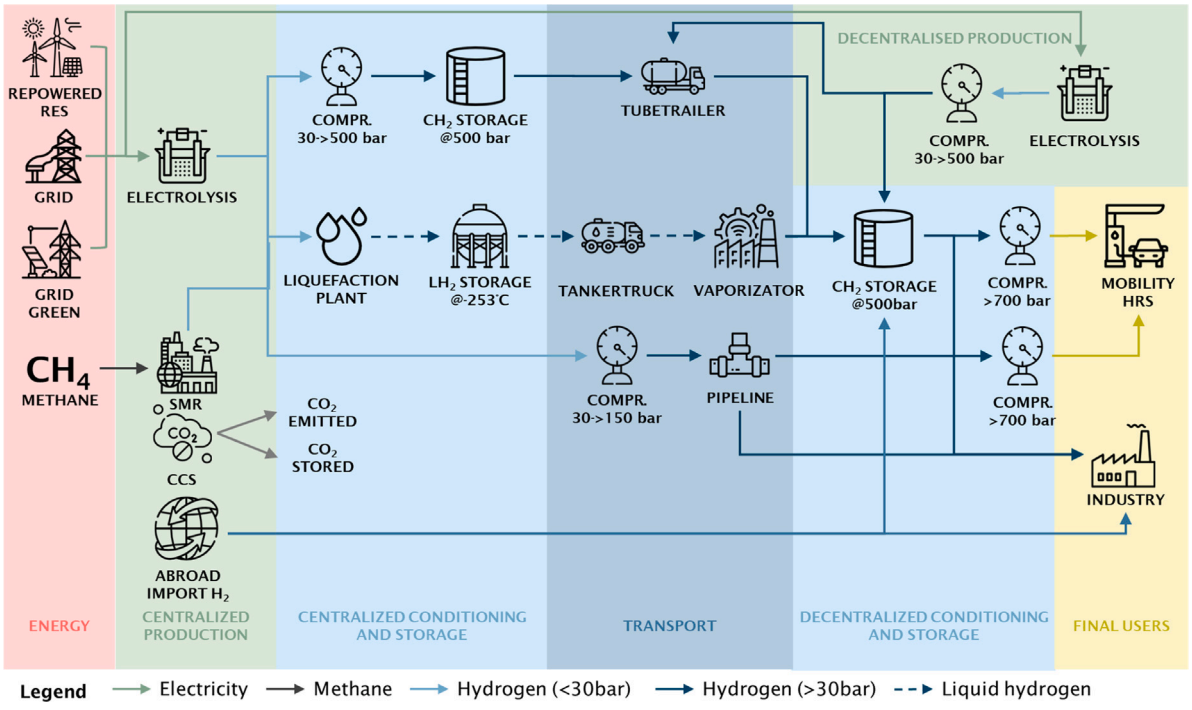

Fig. 7. HSC superstructure - Technological bricks.

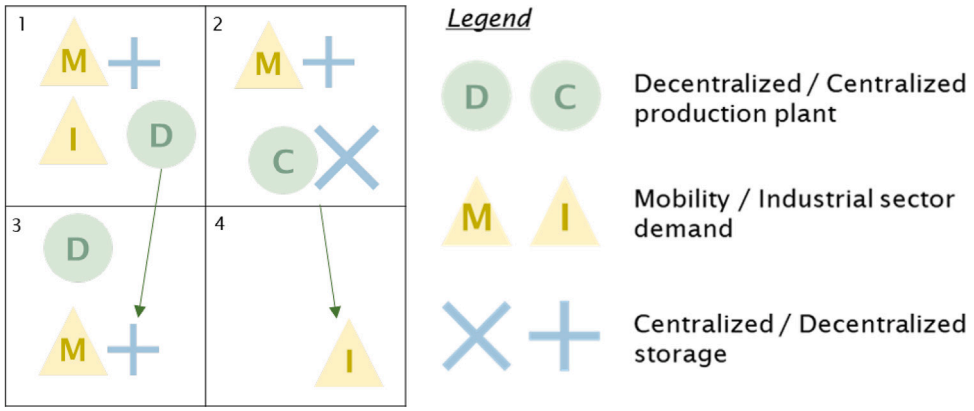

Fig. 8. Sample of HSC development in different grids.

Production plant constraints

For each grid, a total mass flow balance is established. Considering the steady-state nature of the problem, the sum of the hydrogen flow entering grid g ($Q_i lg'gt$) and the total hydrogen produced in grid g (P^T_{igt}) is equal to the sum of the hydrogen flow exiting grid g ($Q_i lgg't$) and the total hydrogen demand of grid g (D^T_{kgt}):

$$P^T_{igt} = \sum_{lg'} (Q_i lgg't - Q_i lg'gt) + \sum_k D'^T_{ikgt} \quad \forall i, g, t \tag{2}$$

A further constraint regards the start year for the installation and operation of large-scale hydrogen production plants (i.e., centralized production plants).

On one hand, the installation of steam reformer plants with CCS systems can only begin once current plants reach the end of their lifecycle. On the other hand, the operation of large-scale electrolyzer plants requires time for industrialization, project development, permitting, and the implementation of regulations such as the Renewable Energy Directive. Given these factors, a conservative approach has been adopted, with steam reformers with CCS and large electrolyzer plants expected to become operational only by 2040.

This study focuses on the degree of centralization in the HSC, which is a key performance indicator (KPI) in the analysis of the upcoming case studies. The degree of centralization is defined as the ratio of hydrogen produced in centralized plants to the total hydrogen produced, as shown in Eq. (3).

$$Centralization\ degree = \frac{\sum_{epigt} PR_{epigt,j=medium,big}}{\sum_{epjigt} PR_{epjigt}} \tag{3}$$

Transport constraints

Two primary modes of transportation have been implemented: road transport lr (involving tanker trucks and tube trailers) and pipeline transport lp. For road transport lr, it is assumed that once a truck is acquired, it can change its route from one period t to another period t'. Conversely, the installation of a pipeline lp remains fixed.

Storage facilities and conditioning constraints

The model incorporates centralized and decentralized storage.

Centralized storage capacity is determined based on daily production capacity and smooths out fluctuations in production, preventing interruptions under low demand. The total storage capacity (S^T_{igt}) is a function of the production rates of centralized plants (PR_{epjigt}) and a multiplicative factor (β):

$$S^T_{igt} = \beta \sum_{epj} PR_{epjigt} \quad \forall i,g,t; \;\; j \neq onsite \tag{4}$$

Decentralized storage capacity is determined by the daily hydrogen supply capacity of the refueling station, as it is integral to the station's operation. No additional variables are introduced for decentralized storage, as its capacity is implicitly accounted for within the station's parameters.

Even though not implemented, Eq. (5) calculates specific energy consumption (w_t) of compressors:

$$w_t = \frac{p_2}{p_1} \cdot 6 \cdot 10^{-17} + \frac{p_2}{p_1} \cdot 0.0585 + 1.095 \tag{5}$$

This equation has been extrapolated from the specific energy consumption of different hydrogen compressors available on the market.

Refueling station constraints

Hydrogen refueling stations have only been implemented for the mobility sector, as it is assumed that industries already using hydrogen have their own storage and supply facilities in place.

To account for the number of refueling stations ($NFS_{f,j,k,g,t}$) of size j for the mobility sector (k = mobility) in grid g at time t, a variable has been introduced. Based on the total hydrogen demand (D^T_{kgt}), the following constraints can be set:

$$\sum_{fj} FSCap^{min}_{fkj} NFS_{fjkgt} \leq D^T_{kgt} \leq \sum_{fj} FSCap^{max}_{fkj} NFS_{fjkgt} \quad \forall g,t; k = mobility \tag{6}$$

where $FSCap^{min}$ and $FSCap^{max}$ are, respectively the minimum and maximum capacity of a refueling station f and size j, supplying hydrogen for the mobility sector. The decentralized storage has been considered together with the refueling station and is sized according to the maximum capacity of the refueling station multiplied by a factor of 2.5.

No decentralized storage has been considered for the industrial sector. The industries considered in this study already use hydrogen and are assumed to have the necessary infrastructure for storing the required amount of hydrogen. As a result, a fictitious storage scenario has been assumed for the industrial sector, with no additional installation costs and unlimited capacity.

Hydrogen mass balance

The relationship between the type of hydrogen produced i (compressed or liquid) and the sector k (mobility or industry) to which the hydrogen is supplied is established through support variables. Constraints are imposed to ensure the balance of total mass flow between the hydrogen produced (P'^T_{ikgt}) at each time period t in each grid g and the total hydrogen consumed (D'^T_{ikgt}).

$$\sum_{ikgt} D'^T_{ikgt} = \sum_{ikgt} P'^T_{ikgt} \quad \forall i,k,g,t \tag{7}$$

Cost objective

The main objective of the model is to optimize the **Levelized Cost of Hydrogen**, denoted as LCOH, expressed in €/kg. The LCOH is calculated as the ratio of the Total System Costs (TSC) of the HSC to the total daily hydrogen demand supplied (D^T_{kgt}) over the entire analysis period. The TSC consists of capital expenditures ($CAPEX_n$), operational expenditures ($OPEX_n$), and maintenance costs (MNT_n). The costs are discounted at a rate of 2% using a discount rate *dr*.

The model considers a period t comprising a certain number of working days *WD*, and each year n is composed of five years.

It is important to note that the variable minimized in the model is the TSC, and the LCOH is subsequently calculated based on the minimized TSC. This approach allows for maintaining linearity in the problem formulation, which would not have been possible by directly optimizing the LCOH.

$$LCOH = \frac{TSC}{\sum_{kgt} D^T_{kgt} \cdot WD \cdot 5} \tag{8}$$

$$TSC = \sum_n CAPEX_n \left(\frac{1}{1+dr}\right)^n + \sum_n WD(OPEX_n + MNT_n)\left(\frac{1}{1+dr}\right)^n \tag{9}$$

Global warming potential objective

To assess the environmental impact of the HSC, this study applies the concept of **GWP**. GWP quantifies the relative contribution of different greenhouse gases to climate change by expressing their impact in terms of carbon dioxide equivalents ($CO_{2_{eq}}$), over a specified time horizon, typically 100 years.

It is important to note that only CO_2 equivalent emissions associated with energy sources are considered in this analysis. The CO_2 impact of the infrastructure itself, including emissions from the construction and maintenance of facilities, is not accounted for. Only direct emissions are considered; consequently, electricity from renewable sources is assumed to be CO_2-free.

The total daily emissions (GWP^T_t) are calculated as the sum of the emissions coming from the production plants (GWP^P_t), storage and conditioning ($GWP^{S\&C}_t$), transport (GWP^{Trans}_t) and supply for mobility (GWP^{Suppy}_t):

$$GWP^T_t = GWP^P_t + GWP^{S\&C}_t + GWP^{Trans}_t + GWP^{Supply}_t \quad \forall t \tag{10}$$

By multiplying then the total daily emissions by the number of working days *WD* and the number of years n in each period t (i.e. 5), the GWP of the whole HSC can be obtained. This GWP value is the objective that has been minimized in the study:

$$GWP = \sum_t GWP^T_t \cdot WD \tag{11}$$

Expected outputs

The objective of the model is to minimize either the overall cost or an environmental criterion. To achieve this, the model encompasses several decision variables that play a crucial role in designing the entire HSC. These variables include:

- Type, number, size, capacity, production rate, and location of hydrogen production and storage units, considering both liquid and compressed storage options.
- Number of transport units and the corresponding flow of hydrogen transported between grids.
- Specification of the sources and quantity of electricity used in the supply chain.
- Number and location of refueling stations dedicated to supplying the hydrogen demand from the mobility sector.

Since the model operates within a temporal framework, each component of the supply chain can be installed at the beginning of each period.

Furthermore, the software ArcGIS is employed to provide improved geographical visualization of the aforementioned variables. ArcGIS, a

geographic information system (GIS) platform, integrates spatial data with analytical tools, enabling visualization and interpretation of the HSC. By leveraging ArcGIS, this study better represents the distribution of production facilities, storage units, transportation routes, and refueling stations, enhancing the understanding of spatial dynamics and optimization opportunities within the hydrogen infrastructure.

4. Selection of the Auvergne-Rhône-Alpes region as a case study

The Auvergne-Rhône-Alpes (ARA) region in France has been selected as the case study due to its strong industrial base, high hydrogen demand, and significant renewable energy potential. Its strategic location as a major transport hub facilitates large-scale hydrogen distribution, while its strong political commitment to hydrogen initiatives reinforces its relevance.

To assess the deployment of HSCs, the developed mathematical model is applied to ARA. The region is represented as a grid where each department is discretized into key urban points. This structured approach ensures a realistic and practical evaluation of infrastructure development.

Geographical approach

The ARA region has been divided into 12 grids, each corresponding to a department. Each department is represented by a single point, located at its major city (the 'Préfecture' in French). The distances between the cities were calculated using Google Maps, and the fastest route was selected for the calculations.

Energy sources

For each grid, the availability of energy sources included in the model and the corresponding costs were sourced from [47]. It is important to note that for the emissions assessment, since only direct emissions are considered, electricity from renewable sources is assumed to be free from CO_2 emissions.

Hydrogen production plants

Three different sizes of electrolyzers were considered: decentralized (1 MW), medium-sized centralized (30 MW), and large-sized centralized (400 MW). However, only the large-sized centralized plant was considered for SMR with CCS.

Investment costs encompass material expenses, stack replacements (twice over the electrolyzer's 20-year lifespan), and balance-of-plant components (e.g., demineralized water unit, power unit, purification unit). They also include indirect manufacturing and installation costs. The cost disparity between decentralized (outdoor) and centralized (indoor) systems arises from differences in materials and components. The model incorporates an economy-of-scale index and periodic cost adjustments, reflecting overall technology cost reductions and a learning rate that decreases costs across all electrolytic solutions (from -36% to −47%).

Another variable that evolves over time and is determined at the beginning of each period is the tax on CO_2 emissions and the costs associated with transporting and storing the captured CO_2 using CCS.

Storage and conditioning

At the outlet of production facilities, hydrogen is considered in its gaseous form at 30 bar. After centralized production, it is either compressed at 500 bar and stored in tanks (CH_2) or liquefied and stored in insulated vessels (LH_2) for transportation via truck in a subsequent step. It is important to note that if the model selects a pipeline as the transport method, no centralized storage will be considered, as the pipeline itself will serve the function of storage.

The investment costs for storage, compressors, and liquefaction plants are considered constant over time, as no significant technological changes or cost reductions are anticipated.

Transportation methods

The transportation methods have been categorized as on-road transport and pipelines. For on-road transports, a tube trailer has been considered for transporting compressed hydrogen at 500 bar, and a tanker truck has been selected for transporting liquid hydrogen.

As a final step, the distances between the grids have been calculated with Google Maps.

Refueling stations

Hydrogen can be delivered to satisfy both the industrial and mobility sectors. For industrial applications, where hydrogen is already extensively used in existing infrastructure, no additional costs for storage and supply points have been considered. It is assumed that hydrogen for transportation (both road and pipeline) will already meet the minimum required purity level (99.5% vol) and pressure for industrial applications (1–10 bar).

Two different sizes of refueling stations have been considered for the mobility sector. Since hydrogen demand is based on the number of light vehicles, the Hydrogen Refueling Station (HRS) is designed to supply hydrogen at 700 bar. In the case of hydrogen transported in liquid form, a vaporizer is included in the conditioning block, with hydrogen assumed to be at 500 bar. When hydrogen is transported via pipeline, the station pressure is assumes to be at 100 bar. The specific energy consumption of the compressors SEC (in kWh/kg_{H_2}) is calculated using Eq. (12) in which β is the compression ratio, defined as the ratio of discharge pressure to inlet (charge) pressure.

$$SEC = 6 \times 10^{-17} \cdot \beta^2 + 0.0585 \cdot \beta + 1.095 \tag{12}$$

Hydrogen demand

The hydrogen demand included in the model is sourced from [47]. At the beginning of the first period (i.e. 2025), the French hydrogen demand is assumed to be roughly 28 tons per day for the mobility sector and slightly over 19 tons per day. By the last analyzed period, hydrogen demand increases to nearly 265 tons per day for mobility and more than 125 tons per day for industrial applications.

Mobility demand is linked to the number of vehicles in each grid, while the industrial demand is only relevant in areas where hydrogen is already in use.

5. Results of the ARA case study

The optimization model has been run with the objectives of minimizing, respectively, the LCOH (Eq. (8)) and the GWP (Eq. (10)) of the supply chain.

The optimization was performed with two constraints: a relative gap of 0.01% for the solution and a time limit of 40,000 s. For the minimization of LCOH, the solution achieved a relative gap of 0.197% after 40,000 s, while in the second optimization, convergence (i.e., relative gap of 0.01%) was reached in less than 60 s.

For better visualization, the results will be presented in two types of figures. The first type displays the cumulative number of installed infrastructures, including production plants, storage facilities, and refueling stations (Fig. 9). The second type shows the connection lines for transported hydrogen (Fig. 10). Due to space limitations, only the final result (i.e., 5th period) is presented in this section, with intermediate results for each period provided in Appendix.

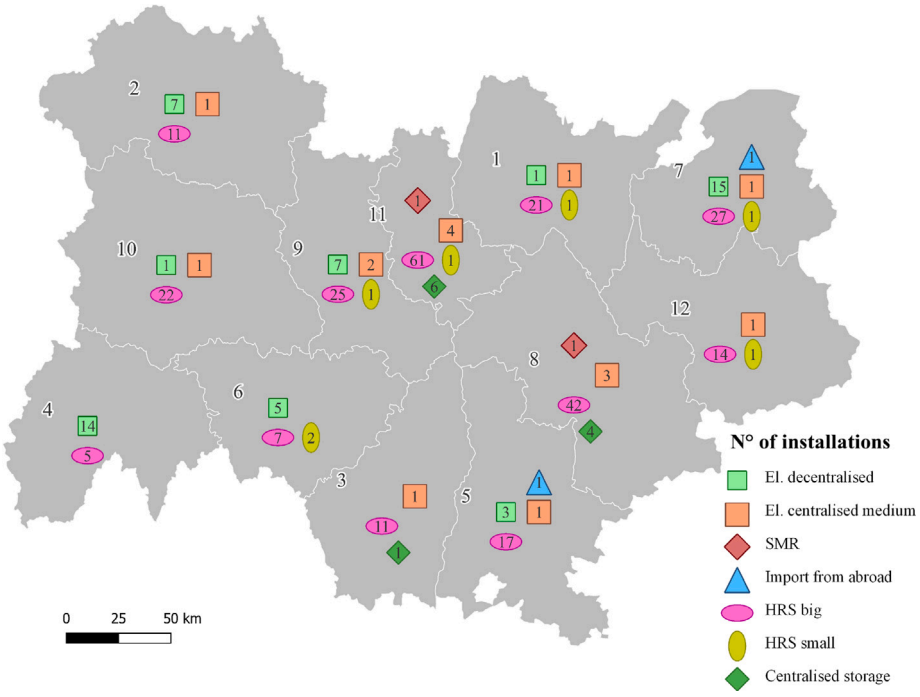

Fig. 9. Number of installations in Auvergne-Rhône-Alpes - 5th period.

5.1. Minimization of total system cost

The results emphasize the interoperability potential of hydrogen technologies within the superstructure. The initial periods are characterized by moderate demand and limited infrastructure, consisting primarily of decentralized electrolysis plants with capacities of 1 MW and 30 MW. As demand increases, additional medium-sized centralized electrolyzers (30 MW) are deployed. In later stages, the superstructure activates additional technological pathways, such as large-scale SMR and high-capacity storage, reflecting the model's ability to dynamically reconfigure the infrastructure over time. The results suggest a preference for SMR plants over electrolysers, with compressed hydrogen in tube trailers as the only transport medium considered.

The final LCOH, calculated as a weighted average over the five periods, is 4.0 €/kg_{H_2}. The cost decreases from 8.9 €/kg_{H_2} in the first period, due to the absence of infrastructure, and stabilizes at 2.4 €/kg in the 5th period after the installation of two SMR plants. Fig. 11 illustrates the cost breakdown by sector, detailing the contributions of primary energy sources, production plants, transport, storage, conditioning, and refueling stations to the final LCOH.

5.2. Minimization of global warming potential

The second optimization, aimed at minimizing emissions in the ARA region, initially produced unrealistic results. The model relied solely on renewable electricity for hydrogen production and pipeline transportation. This approach neglected emissions from auxiliary electricity purchased from the grid without Power Purchase Agreements (PPAs) and allowed pipelines to operate at very low load factors, resulting in an unfeasible LCOH of approximately 1000 €/kg_{H_2}.

To avoid unrealistic solutions, two constraints were added: a minimum load factor of 40% for pipelines and prioritization of electricity from existing plants (with re-powering) over purchasing renewable electricity via PPAs (see Fig. 12).

Table 1
Average cost per period in Auvergne-Rhône-Alpes in the Hydrogen + scenario, emission minimization alternative.

Period	1	2	3	4	5	Weighted average
LCOH min. - CO_2 emissions [$\frac{g_{CO_{2eq}}}{kg_{H_2}}$]	1642	1477	1630	1680	1539	1594
GWP min. - CO_2 emissions [$\frac{g_{CO_{2eq}}}{kg_{H_2}}$]	136	159	158	158	147	153

Compared to the LCOH minimization scenario (Section 5.1), a higher number of centralized production plants are installed in the first period (8 vs. 3), while hydrogen transport is entirely avoided over the whole analysis period. Although two large-scale centralized plants are still deployed, they are now electrolyzer-based (400 MW), resulting in a lower environmental impact.

5.3. Comparison of results between the LCOH and GWP minimization

To minimize emissions during the analyzed period, more costly options are chosen for energy sources, production plants, and transportation methods.

As a result, the average hydrogen cost is approximately 2 €/kg higher than in the LCOH minimization analysis, as shown in Fig. 13. However, this approach leads to a tenfold reduction in the weighted average specific emissions, dropping from 1539 $g_{CO_{2eq}}/kg_{H_2}$ to only 153 $g_{CO_{2eq}}/kg_{H_2}$, as shown in Table 1. Residual emissions in the GWP minimization arise from auxiliary electricity consumption for hydrogen conditioning, which cannot be avoided within the model structure.

Looking at similar studies assessing LCOH at regional or national scales, values typically range from about 2 €/kg_{H_2} to 7 €/kg_{H_2} [53, 54], depending on technology, location, and scenario assumptions. The results obtained in this study, ranging from 4.0 €/kg_{H_2} to 6.2

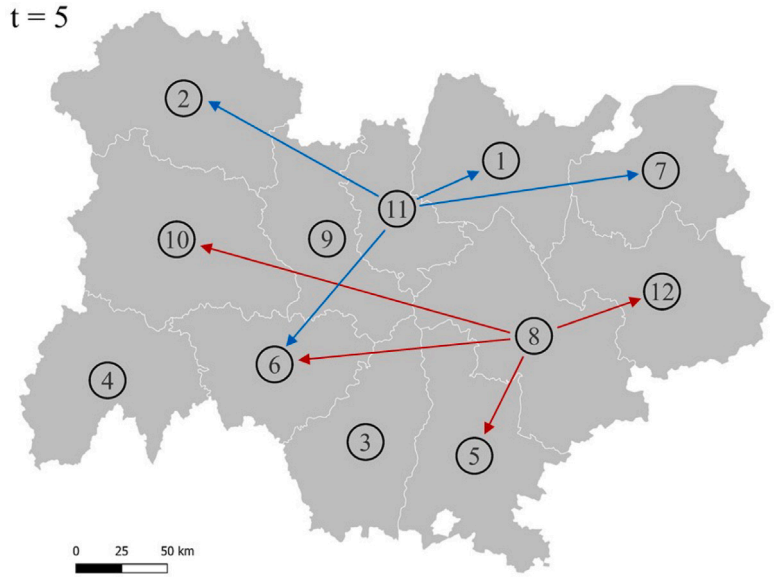

Fig. 10. Hydrogen transportation in Auvergne-Rhône-Alpes among the different grids - 5th period.

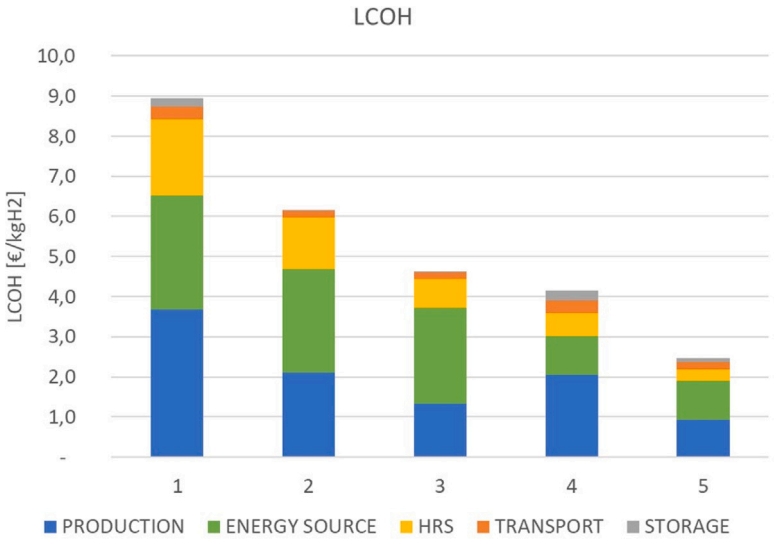

Fig. 11. LCOH cost breakdown per sector in Auvergne-Rhône-Alpes [€/kg_{H_2}].

€/kg_{H_2} over the period 2025–2050, are consistent with these orders of magnitude. However, since no dedicated studies exist for the ARA region in France and because design, technical, and economic inputs differ among available works, a precise comparison is not possible.

6. Sensitivity analysis of the ARA case study

This section presents a sensitivity analysis of the Auvergne-Rhône-Alpes (ARA) case study, aiming to evaluate how fluctuations in key parameters, specifically hydrogen demand, capital expenditures (CAPEX), and primary energy costs, influence the design and economic performance of the Hydrogen Supply Chain (HSC), compared to the previously introduced Base Case Study (BCS).

6.1. Impact of hydrogen demand penetration

To assess the implications of a slower market uptake, a scenario based on the RTE "Reference" scenario was implemented, where the 2050 demand is limited to 1700 kton/year, compared to the 4000 kton/year of the BCS, which relies on the "Hydrogen+" scenario of RTE. In the initial stages (Period 1), the reduced demand favors a more decentralized configuration, primarily utilizing 1 MW electrolyzer plants. Notably, while a medium-sized centralized plant is established early in specific grids to serve neighboring demand, the overall degree of centralization remains lower than the BCS (64% vs. 73%) during the first three periods.

As the simulation progresses into the fourth period, the model shifts toward large-scale centralized solutions, such as Steam Methane Reforming (SMR), to achieve economies of scale. However, a critical finding is that under lower demand, these large-scale plants operate at significantly reduced load factors (e.g., 35% capacity in Period 4). Consequently, a lower demand scenario exhibits lower costs initially due to reduced infrastructure requirements, but the long-term Levelized Cost of Hydrogen (LCOH) becomes higher than the BCS once installation costs are absorbed (see Table 2). Specifically, in Period 4, the LCOH is 14.4% higher than the BCS.

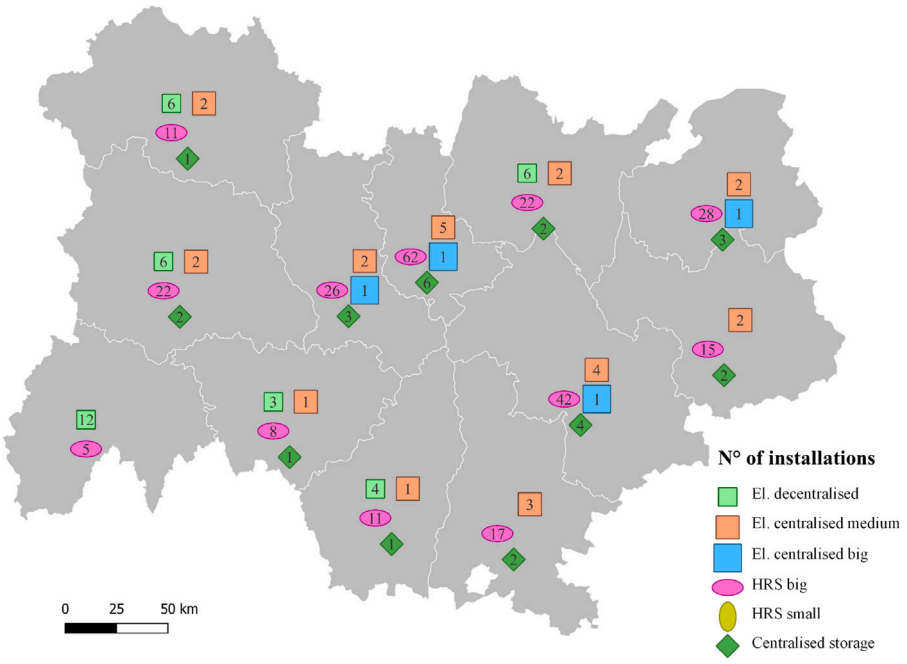

Fig. 12. Installations Auvergne-Rhône-Alpes with minimized emissions- 5th period.

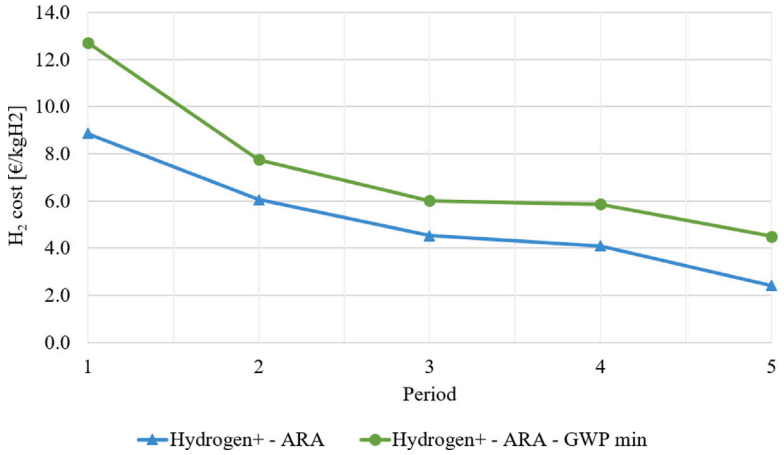

Fig. 13. LCOH comparison for different objective functions.

6.2. Influence of financial incentives: Production vs. Infrastructure

Two scenarios were conducted to evaluate the impact of a 20% reduction in CAPEX, targeting either production plants (electrolyzers) or refueling stations (HRS), in order to understand which echelon has a greater effect on the final LCOH.

- **Production Incentives:** Reducing electrolyzer costs promotes a more fragmented and decentralized system. In the first period, the number of decentralized plants nearly doubles compared to the BCS (60 vs. 33), leading to a centralization degree of only 50%. This shift reduces the necessity for road transport in the early stages, although the long-term weighted average LCOH decreases by a modest 1.6%.
- **Infrastructure Incentives:** Conversely, applying the same 20% reduction to HRS costs proved significantly more effective, yielding a 5.5% reduction in the weighted average LCOH. Interestingly, this cost reduction does not alter the physical design of the HSC, which remains identical to the BCS. The higher impact is explained by the fact that refueling stations represent the dominant share of total investment costs, accounting for 26% to 88.4% of the LCOH depending on the period.

6.3. Energy price volatility: The post-war scenario

The sensitivity to primary energy costs was tested by simulating the peak prices observed following the Russia-Ukraine conflict, where electricity and natural gas costs increased by factors of 3 and 4, respectively.

This scenario necessitates a radical reconfiguration of the HSC. The system moves toward the maximum utilization of local re-powered renewable energy sources (RES) to avoid the high costs of grid-sourced electricity. While this strategy mitigates some costs, it necessitates a massive expansion of the transport network; the volume of hydrogen transported via truck increases by four- to eightfold compared to the BCS. Economically, this results in a weighted average LCOH of 6.2 €/kg, a 55.3% increase over the base case. Furthermore, direct greenhouse gas (GHG) emissions rise due to the intensified diesel consumption of the truck fleet required for inter-grid distribution.

Table 2
LCOH comparison between the BCS and sensitivity analyses [€/kgH2].

Scenario	P1	P2	P3	P4	P5	Weighted Avg.
BCS (Base Case)	8.9	6.1	4.5	4.1	2.4	4.0
S.A.1 - Lower Demand	8.5	5.1	3.6	4.7	2.6	4.0
S.A.2 - CAPEX Prod. (−20%)	8.3	6.0	4.4	4.0	2.4	3.9
S.A.3 - CAPEX HRS (−20%)	8.3	5.7	4.3	3.9	2.3	3.8
S.A.4 - Energy Costs	9.3	8.4	8.3	5.8	4.4	6.2

6.4. Comparative summary of results

The results of these analyses, summarized in Table 2, highlight that while demand levels dictate the long-term utilization of large-scale assets, the cost of the final delivered hydrogen is most sensitive to infrastructure costs,particularly refueling stations, and the volatility of primary energy prices.

Ultimately, these findings emphasize that local RES integration serves as a buffer against external energy crises, even if it requires more complex logistical planning. Moreover, strategic planning should prioritize optimizing refueling infrastructure to achieve the most significant reductions in hydrogen delivery costs.

7. Conclusions

This work presents a comprehensive superstructure-based model for HSC design built upon a flexible and unified framework that integrates all major configurations — centralized, decentralized, and hybrid — for both hydrogen production and storage. Unlike previous approaches that often examine a single layout, this model supports diverse architectures with various interoperable hydrogen technologies and allows dynamic inter-site interactions, especially between decentralized production units. This feature enhances system flexibility, which is particularly valuable during early deployment phases characterized by fluctuating demand and capacity imbalance.

The superstructure explicitly models six interconnected echelons: primary energy sourcing, hydrogen production, conditioning and centralized storage, distribution, conditioning and decentralized storage, and final use. It captures all relevant stakeholder interactions, technological options, and logistical choices. Hydrogen can be produced through electrolysis (of varying scales), SMR with carbon capture and storage, or imports. Once conditioned and stored, hydrogen is distributed via road or pipelines to meet demand, primarily from the mobility and industrial sectors.

To validate the model, a real-world case study was conducted in the Auvergne-Rhône-Alpes region (France), comparing two optimization objectives: minimizing the LCOH and minimizing the GWP. In the cost-minimization scenario, SMR-based centralized plants were favored, resulting in 4.0 €/kg_{H_2} and 1594 $g_{CO_{2_{eq}}}/kg_{H_2}$. In contrast, minimizing emissions favored 400 MW electrolyzers powered by renewable electricity, achieving a carbon footprint of 153 $g_{CO_{2_{eq}}}/kg_{H_2}$ at a higher cost of 6.2 €/kg. These scenarios also revealed trade-offs in transport design—tube trailers were used in the LCOH case, while inter-grid transport was avoided in the GWP case.

Overall, the four sensitivity analyses indicate that, while demand levels primarily influence the long-term utilization of large-scale assets, the cost of hydrogen is most strongly driven by infrastructure-related expenditures, particularly those associated with refueling stations, and by the volatility of primary energy prices. The results further highlight that the integration of local renewable energy sources can effectively mitigate exposure to external energy crises, albeit at the cost of increased logistical complexity. Consequently, strategic planning efforts should focus on optimizing refueling infrastructure, as this represents the most impactful lever for reducing hydrogen delivery costs.

Table A.3
Degree of centralization in the Auvergne-Rhône-Alpes region per period in the Hydrogen+ scenario, emission minimization alternative.

Period	1	2	3	4	5
Degree of centralization - Cost minimization	79%	91%	95%	96%	97%
Degree of centralization - Emission minimiz.	73%	94%	90%	98%	97%

Table A.4
Average cost per period in Auvergne-Rhône-Alpes in the Hydrogen+ scenario, emission minimization alternative.

Period	1	2	3	4	5	Weighted average
LCOH min. - CO_2 emissions $[\frac{g_{CO_{2eq}}}{kg_{H_2}}]$	1642	1477	1630	1680	1539	1594
GWP min. - CO_2 emissions $[\frac{g_{CO_{2eq}}}{kg_{H_2}}]$	136	159	158	158	147	153

Importantly, the framework is scalable and adaptable to different territorial levels — from regional to national — and supports sectoral differentiation of hydrogen uses. By combining techno-economic optimization with environmental assessment, the model offers a valuable decision-support tool to guide the deployment of low-carbon, cost-effective HSCs.

Future research directions include extending the superstructure to incorporate alternative hydrogen carriers such as LOHC and Ammonia, which offer promising options for long-distance and high-capacity transport. These vectors can be modeled as additional interoperable pathways within the existing framework, enabling richer comparisons and broader deployment strategies. Moreover, incorporating uncertainty, particularly in renewable generation availability and hydrogen demand profiles, through stochastic or robust optimization techniques, would enhance the robustness of the decisions.

CRediT authorship contribution statement

Renato Luise: Writing – original draft, Methodology, Investigation, Conceptualization. **Catherine Azzaro-Pantel:** Writing – review & editing, Conceptualization. **Annabelle Brisse:** Validation, Conceptualization.

Declaration of competing interest

The authors declare that they have no known competing financial interests or personal relationships that could have appeared to influence the work reported in this paper.

Appendix. Results of the ARA case study

A.1. Minimization of total system cost

See Figs. A.14 and A.15.

A.2. Minimization of GWP

See Figs. A.16–A.18 and Tables A.3 and A.4.

Data availability

Data will be made available on request.

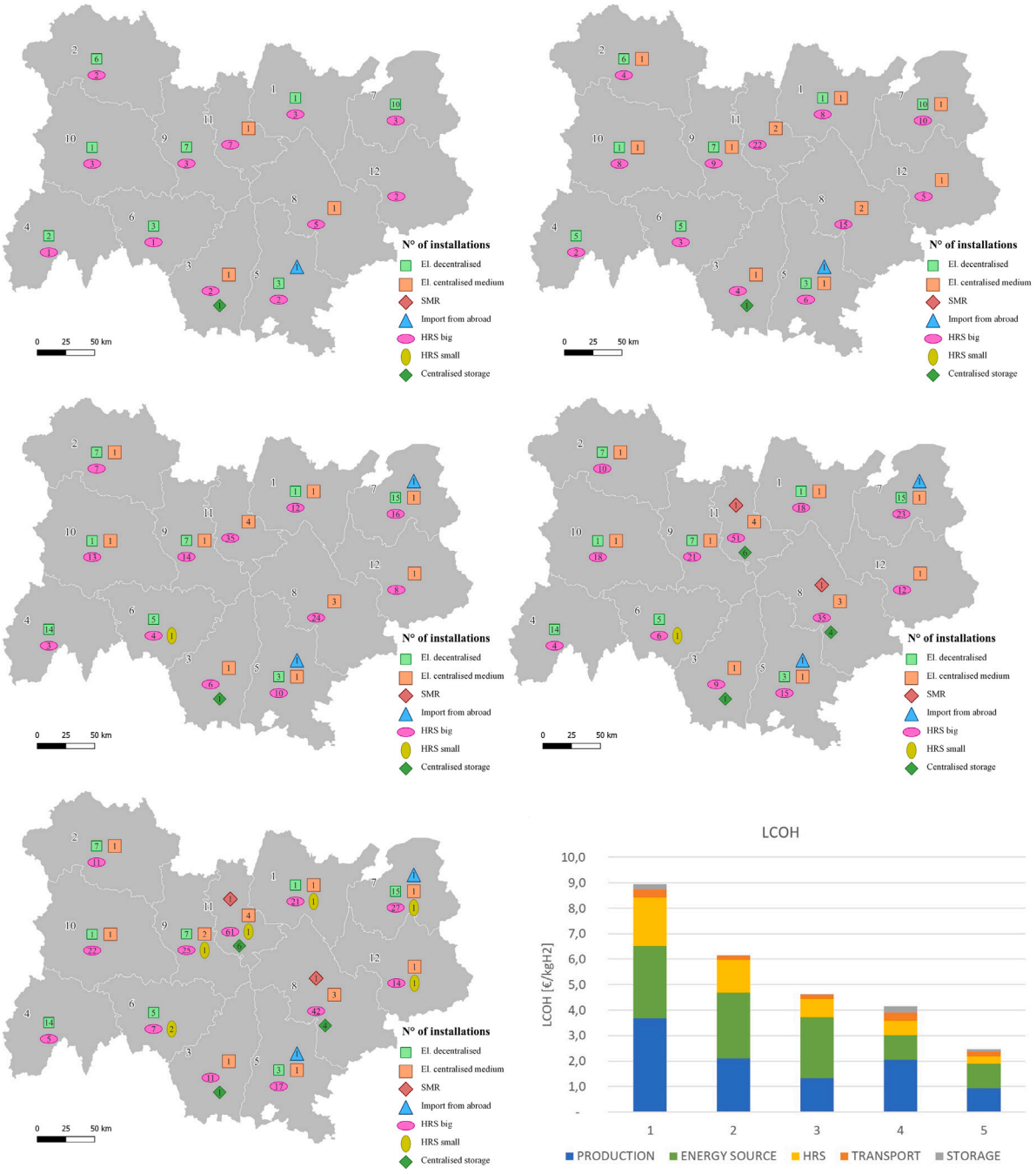

Fig. A.14. Installations in the Auvergne-Rhône-Alpes region in the Hydrogen+ scenario, minimizing total yearly system cost, periods 1 to 5.

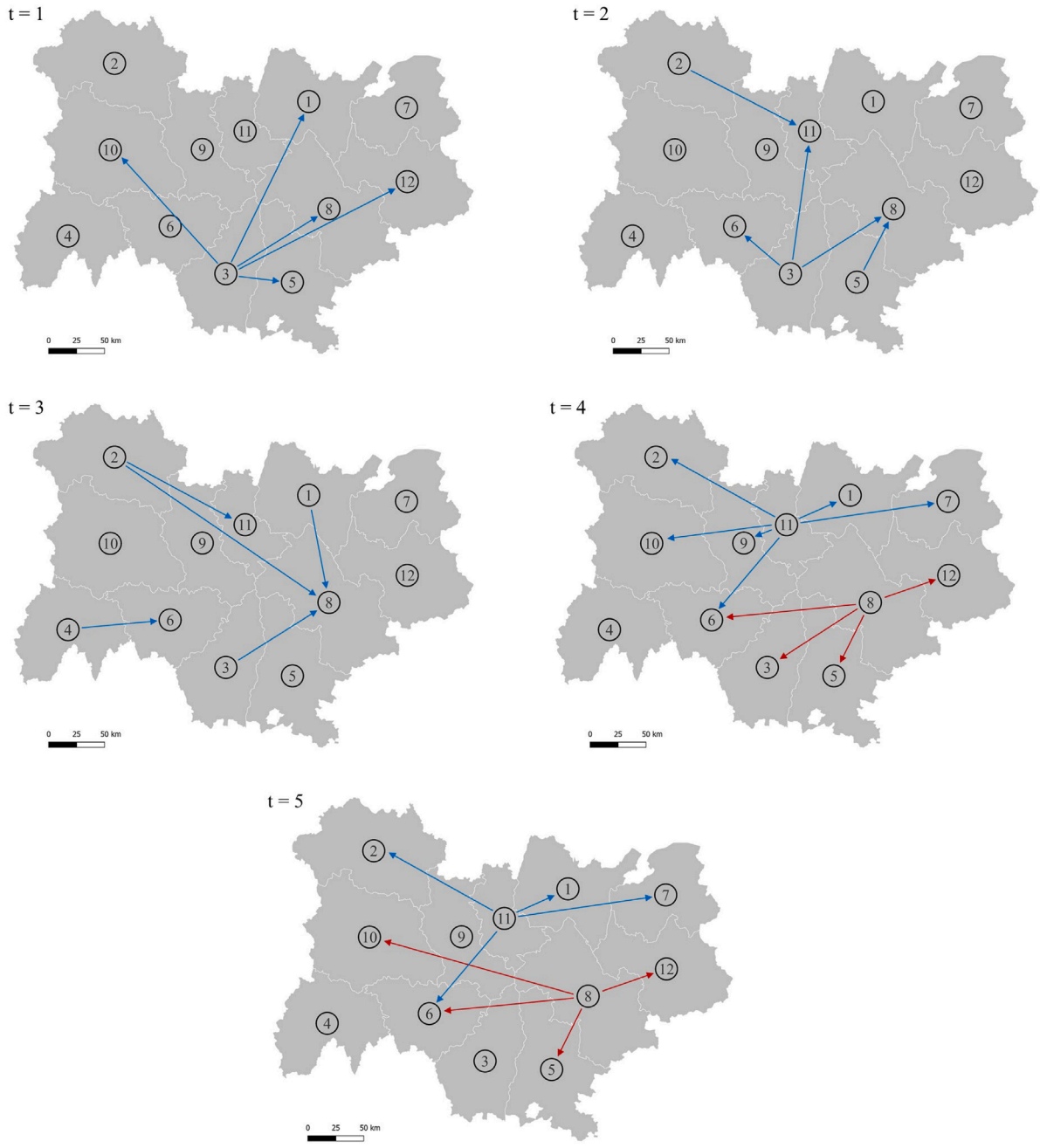

Fig. A.15. Hydrogen transportation routes in the Auvergne-Rhône-Alpes region in the Hydrogen+ scenario.

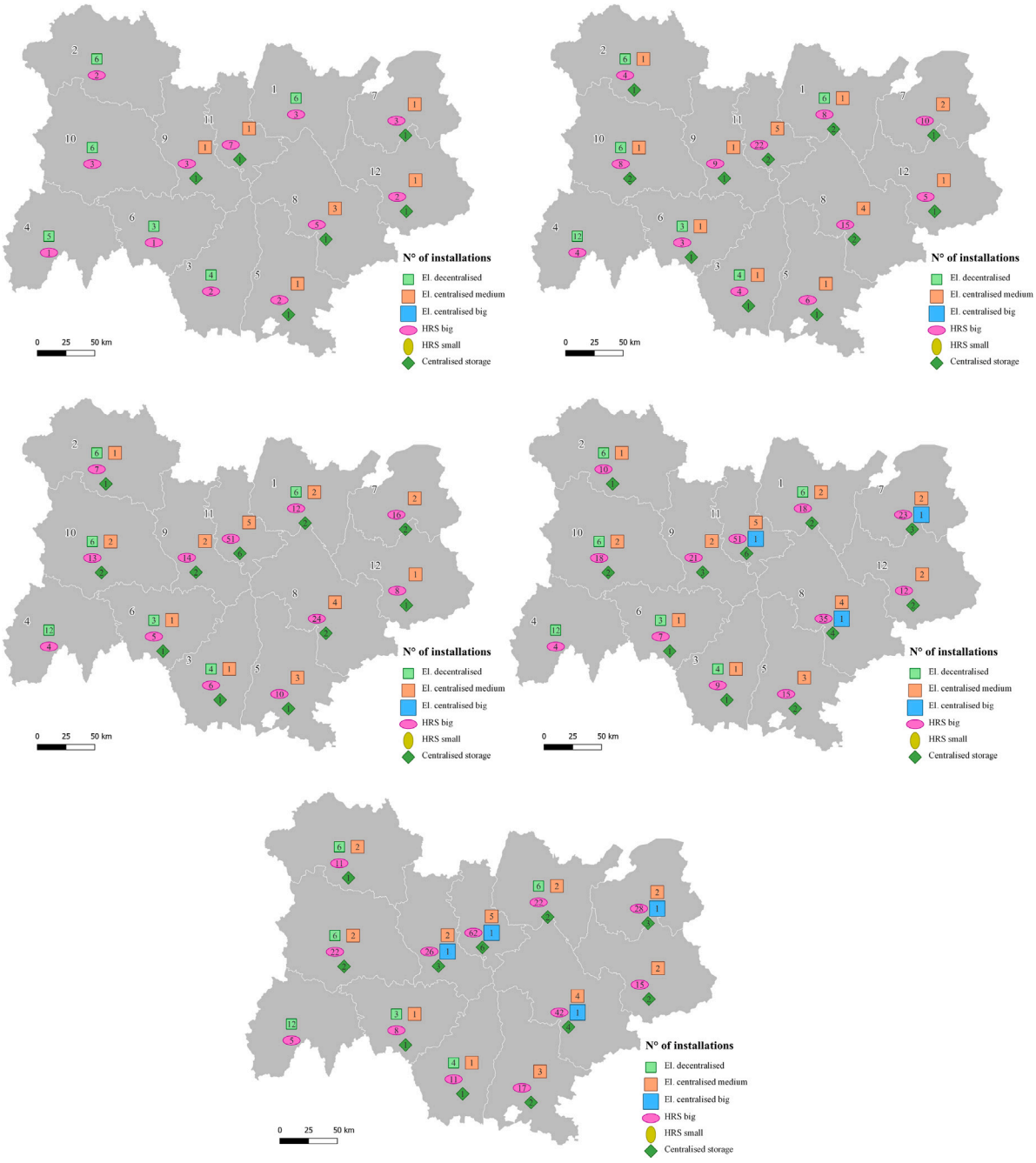

Fig. A.16. Installations in the Auvergne-Rhône-Alpes region in the Hydrogen+ scenario, emission minimization, periods 1 to 5.

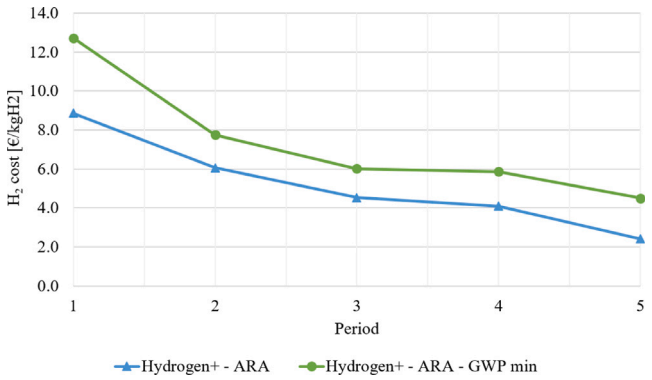

Fig. A.17. Comparison of final hydrogen costs between cost minimization and emission minimization case studies in the Hydrogen+ scenario.

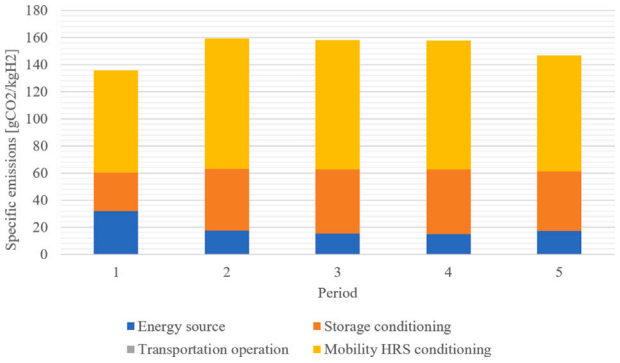

Fig. A.18. Specific emissions in the Auvergne-Rhône-Alpes regionin the Hydrogen+ scenario, emission minimization alternative.

References

[1] International Energy Agency. Global hydrogen review 2024. 2024, https://www.iea.org.

[2] Fuel Cells and Hydrogen Joint Undertaking. A sustainable pathway for the European energy transition: Hydrogen roadmap Europe. 2020, http://dx.doi.org/10.2843/249013.

[3] Busch T, et al. The hydrogen supply chain — a comprehensive literature review incorporating purity analysis. Int J Hydrog Energy 2025;164:149367. http://dx.doi.org/10.1016/j.ijhydene.2025.149367.

[4] Bozzolo Lueckel FB, Monaghan RFD, Lynch MA. Hydrogen supply chain modelling at energy system scale: a review. Renew Sustain Energy Rev 2025;210:115218. http://dx.doi.org/10.1016/j.rser.2024.115218.

[5] Sizaire P, Lin B, Gencer E. A novel hydrogen supply chain optimization model: case study of texas and Louisiana. Int J Hydrog Energy 2024;78:401–20. http://dx.doi.org/10.1016/j.ijhydene.2024.06.236.

[6] Pinsky Roxanne, et al. Comparative review of hydrogen production technologies for nuclear hybrid energy systems. Prog Nucl Energy 2020;123:103317. http://dx.doi.org/10.1016/j.pnucene.2020.103317.

[7] Tian M, Zhong S, Al Ghassani MAM. Simulation and feasibility assessment of a green hydrogen supply chain: a case study in Oman. Env Sci Pollut Res 2025;32:13313–28. http://dx.doi.org/10.1007/s11356-024-32563-z.

[8] Steidl S, Peer RA M, Alhamwi A. GIS-based modelling of hydrogen integration in urban energy systems: a systematic review. Curr Sustain Renew Energy Rep 2024;11:85–94. http://dx.doi.org/10.1007/s40518-024-00242-9.

[9] Fang H, et al. Spatial optimization strategies for China's hydrogen infrastructure industry chain. Energy Rep 2024;12:4523–38. http://dx.doi.org/10.1016/j.egyr.2024.10.018.

[10] Oliveira VESF, do Carmo BB T, da Costa Fontes FF. Hydrogen supply chains: modeling challenges and sustainability gaps. Appl Energy 2025;401:126827. http://dx.doi.org/10.1016/j.apenergy.2025.126827.

[11] Almansoori A, Shah N. Design and operation of a future hydrogen supply chain: Snapshot model. Chem Eng Res Des 2006;84(6):423–38. http://dx.doi.org/10.1205/cherd.05193.

[12] Almansoori A, Shah N. Design and operation of a future hydrogen supply chain: Multi-period model. Int J Hydrog Energy 2009;34(19):7883–97. http://dx.doi.org/10.1016/j.ijhydene.2009.07.109.

[13] Mencarelli Luca, et al. A review on superstructure optimization approaches in process system engineering. Comput Chem Eng 2020;136:106808. http://dx.doi.org/10.1016/j.compchemeng.2020.106808.

[14] Luise Renato, Brisse Annabelle, Azzaro-Pantel Catherine. Centralised vs. decentralised production and storage: optimal design of a decarbonised hydrogen supply chain with multiple end uses. In: Computer aided chemical engineering. Elsevier; 2021, http://dx.doi.org/10.1016/B978-0-323-88506-5.50275-8.

[15] Luise Renato, Brisse Annabelle, Azzaro-Pantel Catherine. Review: Analysis of superstructures for hydrogen supply chain modeling. In: Computer aided chemical engineering. Elsevier; 2023, p. 165–81. http://dx.doi.org/10.1016/B978-0-323-99514-6.00017-0.

[16] Yang Mingyang, Liu Linlin, Du Jian. Design of hydrogen supply chain networks for cross-regional distribution. Ind Eng Chem Res 2025. http://dx.doi.org/10.1021/acs.iecr.4c03989.

[17] Efthymiadou Margarita E, Charitopoulos Vassilis M, Papageorgiou Lazaros G. Optimization approach for hydrogen infrastructure planning under uncertainty. Ind Eng Chem Res 2025;64(14):7431–51. http://dx.doi.org/10.1021/acs.iecr.4c04211.

[18] Almansoori A, Shah N. Design and operation of a stochastic hydrogen supply chain network under demand uncertainty. Int J Hydrog Energy 2012;37(5). http://dx.doi.org/10.1016/j.ijhydene.2011.11.091.

[19] Carrera Guilarte Eduardo. A methodological design framework for hybrid power-to-methane and power-to-hydrogen supply chains: application to occitania region, France [PhD thesis], Toulouse, France: Institut National Polytechnique de Toulouse (INPT); 2021, PhD thesis.

[20] De-Le'on Almaraz Sof'ia, et al. Assessment of mono- and multi-objective optimization to design a hydrogen supply chain. Int J Hydrog Energy 2013;38(33). http://dx.doi.org/10.1016/j.ijhydene.2013.07.059.

[21] Nunes Paula, et al. Design of a hydrogen supply chain with uncertainty. Int J Hydrog Energy 2015;40(46). http://dx.doi.org/10.1016/j.ijhydene.2015.10.015.

[22] Sabio Nagore, et al. Strategic planning with risk control of hydrogen supply chains for vehicle use under uncertainty in operating costs: A case study of Spain. Int J Hydrog Energy 2010;35(13). http://dx.doi.org/10.1016/j.ijhydene.2010.04.010.

[23] Won Wangyun, et al. Design and operation of renewable energy sources based hydrogen supply system: Technology integration and optimization. Renew Energy 2017;103. http://dx.doi.org/10.1016/j.renene.2016.11.038.

[24] Woo Young-Bin, Kim Byung Soo. A genetic algorithm-based matheuristic for hydrogen supply chain network problem with two transportation modes and replenishment cycles. Comput Ind Eng 2019;127. http://dx.doi.org/10.1016/j.cie.2018.11.027.

[25] Kim Minsoo, Kim Jiyong. Optimization model for the design and analysis of an integrated renewable hydrogen supply (IRHS) system: Application to Korea's hydrogen economy. Int J Hydrog Energy 2016;41(38). http://dx.doi.org/10.1016/j.ijhydene.2016.07.079.

[26] Kamarudin SK, et al. Synthesis and optimization of future hydrogen energy infrastructure planning in Peninsular Malaysia. Int J Hydrog Energy 2009;34(5). http://dx.doi.org/10.1016/j.ijhydene.2008.12.086.

[27] Gueler Mehmet Gueray, Geçici Ebru, Erdoğan Ahmet. Design of a future hydrogen supply chain: A multi period model for Turkey. Int J Hydrog Energy 2021;46(30). http://dx.doi.org/10.1016/j.ijhydene.2020.09.018.

[28] Lahnaoui Amin, et al. Optimizing hydrogen transportation system for mobility by minimizing the cost of transportation via compressed gas truck in North Rhine-Westphalia. Appl Energy 2018;223. http://dx.doi.org/10.1016/j.apenergy.2018.03.099.

[29] Samsatli Sheila, Staffell Iain, Samsatli Nouri J. Optimal design and operation of integrated wind-hydrogen-electricity networks for decarbonising the domestic transport sector in Great Britain. Int J Hydrog Energy 2016;41(1). http://dx.doi.org/10.1016/j.ijhydene.2015.10.032.

[30] Kazi Monzure-Khoda, et al. Green hydrogen for industrial sector decarbonization: Costs and impacts on hydrogen economy in Qatar. Comput Chem Eng 2021;145. http://dx.doi.org/10.1016/j.compchemeng.2020.107144.

[31] Moreno-Benito Marta, Agnolucci Paolo, Papageorgiou Lazaros G. Towards a sustainable hydrogen economy: Optimisation-based framework for hydrogen infrastructure development. Comput Chem Eng 2017;102. http://dx.doi.org/10.1016/j.compchemeng.2016.08.005.

[32] Seo Seung-Kwon, Yun Dong-Yeol, Lee Chul-Jin. Design and optimization of a hydrogen supply chain using a centralized storage model. Appl Energy 2020;262. http://dx.doi.org/10.1016/j.apenergy.2019.114452.

[33] Kim Minsoo, Kim Jiyong. An integrated decision support model for design and operation of a wind-based hydrogen supply system. Int J Hydrog Energy 2017;42(7). http://dx.doi.org/10.1016/j.ijhydene.2016.10.129.

[34] Ochoa Robles Jesus, et al. Optimal design of a sustainable hydrogen supply chain network: Application in an airport ecosystem. ACS Sustain Chem Eng 2019;7. http://dx.doi.org/10.1021/acssuschemeng.9b02620.

[35] Yang Christopher, Ogden Joan M. Renewable and low carbon hydrogen for California – modeling the long term evolution of fuel infrastructure using a quasi-spatial TIMES model. Int J Hydrog Energy 2013;38(11). http://dx.doi.org/10.1016/j.ijhydene.2013.01.195.

[36] Reuß Markus, et al. A hydrogen supply chain with spatial resolution: Comparative analysis of infrastructure technologies in Germany. Appl Energy 2019;247. http://dx.doi.org/10.1016/j.apenergy.2019.04.064.
[37] Lahnaoui Amin, et al. Optimizing hydrogen transportation system for mobility via compressed hydrogen trucks. Int J Hydrog Energy 2019;44(35). http://dx.doi.org/10.1016/j.ijhydene.2018.10.234.
[38] Yang C, Ogden J. Determining the lowest-cost hydrogen delivery mode. Int J Hydrog Energy 2007;32(2). http://dx.doi.org/10.1016/j.ijhydene.2006.05.009.
[39] Talebian Hoda, Herrera Omar E, Mérida Walter. Spatial and temporal optimization of hydrogen fuel supply chain for light duty passenger vehicles in British Columbia. Int J Hydrog Energy 2019;44(47):25939–56. http://dx.doi.org/10.1016/j.ijhydene.2019.07.218.
[40] Li Lei, Manier Hervé, Manier Marie-Ange. Integrated optimization model for hydrogen supply chain network design and hydrogen fueling station planning. Comput Chem Eng 2020;134. http://dx.doi.org/10.1016/j.compchemeng.2019.106683.
[41] Ochoa Robles Jesus, Azzaro-Pantel Catherine, Aguilar-Lasserre Alberto. Optimization of a hydrogen supply chain network design under demand uncertainty by multi-objective genetic algorithms. Comput Chem Eng 2020;140:106853. http://dx.doi.org/10.1016/j.compchemeng.2020.106853.
[42] Ochoa Robles Jesus, De-León Almaraz Sofia, Azzaro-Pantel Catherine. Optimization of a hydrogen supply chain network design by multi-objective genetic algorithms. 2016, http://dx.doi.org/10.1016/B978-0-444-63428-3.50139-9.
[43] dena. Marktverfuegbare innovationen zur steigerung der energieeffizienz in der industrie zusammenfassung. 2017, URL: www.dena.de.
[44] française République. Ordonnance n° 2021-167 du 17 février 2021 relative à l'hydrogène. J off République française 2021. Dernière modification: 29 juillet 2021.
[45] française République. Arrêté du 1er juillet 2024 précisant le seuil d'émissions de gaz à effet de serre et la méthodologie pour qualifier l'hydrogène comme renouvelable ou bas-carbone. J off République française 2024. JORF n°0157 du 4 juillet 2024, NOR: ECOR2323734A; dernière mise à jour: 5 juillet 2024.
[46] Ericsson Karin. Biogenic carbon dioxide as feedstock for production of chemicals and fuels: a techno-economic assessment with a European perspective [PhD thesis], Lund, Sweden: Lunds universitet, Miljoe- och energisystem, LTH; 2017, PhD thesis.
[47] Luise Renato, Brisse Annabelle, Azzaro-Pantel Catherine. Paving the way for low-carbon hydrogen supply chain deployment by exploring the potential of renewable energies and multisectoral hydrogen demand: Case study of France. Renew Energy Focus 2024;50:100613. http://dx.doi.org/10.1016/j.ref.2024.100613.
[48] Konda NVSN Murthy, Shah Nilay, Brandon Nigel P. Optimal transition towards a large-scale hydrogen infrastructure for the transport sector: The case for the Netherlands. Int J Hydrog Energy 2011;36(8). http://dx.doi.org/10.1016/j.ijhydene.2011.01.104.
[49] International Energy Agency. Global hydrogen review 2021. 2021, URL: www.iea.org/t&c/.
[50] De-León Almaraz Sofia. Multi-objective optimisation of a hydrogen supply chain [PhD thesis], Toulouse, France: Institut National Polytechnique de Toulouse (INPT); 2014, PhD thesis.
[51] Riera Jefferson A, Lima Ricardo M, Knio Omar M. A review of hydrogen production and supply chain modeling and optimization. Int J Hydrog Energy 2023;48(37):13731–55. http://dx.doi.org/10.1016/j.ijhydene.2022.12.242.
[52] Cantú Medrano Victor Hugo. Métaheuristiques et matheuristiques pour des problèmes d'optimisation multi-objectifs en génie des procédés: application à la conception d'une chaîne logistique «hydrogène » [PhD thesis], Toulouse, France: Institut National Polytechnique de Toulouse (INPT); 2021, PhD thesis.
[53] Kostlbacher Jürgen, et al. Application of an electrolysis system model for techno-economic optimization of hydrogen production in industry-based case studies. Int J Hydrog Energy 2025;138:1144–62. http://dx.doi.org/10.1016/j.ijhydene.2025.03.291.
[54] Mendler Friedrich, et al. Optimisation of possible transformation pathways for hydrogen valleys: Case study southern Upper Rhine Region. Int J Hydrog Energy 2025;138:985–1003. http://dx.doi.org/10.1016/j.ijhydene.2025.05.198.